Research Article | Vol. 25, No. 20 | 2 Oct 2017 | OPTICS EXPRESS 23663
Optics EXPRESS

Experimental demonstration of multi-cavity optoelectronic oscillation over a multicore fiber

SERGI GARCÍA* AND IVANA GASULLA

ITEAM Research Institute, Universitat Politècnica de València, Camino de Vera, 46022, Valencia, Spain
**sergarc3@iteam.upv.es*

Abstract: We report, for the first time to our knowledge, the experimental demonstration of multi-cavity optoelectronic oscillators where the cavities are provided by the different cores of a multicore fiber. We implemented two multi-cavity architectures over a 20-m-long 7-core fiber link: unbalanced dual-cavity oscillation (the cavity lengths are a multiple of a reference value) and multi-cavity Vernier oscillation (the cavity lengths are slightly different). Since all the cavities are hosted under a single fiber cladding and are subject to the same environmental and mechanical conditions, optoelectronic oscillators built upon multicore fibers benefit from improved performance stability as compared to independent singlemode fiber cavities.

OCIS codes: (060.2360) Fiber optics links and subsystems; (060.5625) Radio frequency photonics; (140.4780) Optical resonators; (230.0250) Optoelectronics; (230.4910) Oscillators.

References and links

1. D. J. Richardson, J. M. Fini, and L. E. Nelson, "Space division multiplexing in optical fibers," Nat. Photonics **7**(5), 354–362 (2013).
2. J. Capmany, J. Mora, I. Gasulla, J. Sancho, J. Lloret, and S. Sales, "Microwave photonic signal processing," J. Lightwave Technol. **31**(4), 571–586 (2013).
3. I. Gasulla and J. Capmany, "Microwave photonics applications of multicore fibers," IEEE Photonics J. **4**(3), 877–888 (2012).
4. S. Garcia and I. Gasulla, "Design of Heterogeneous Multicore Fibers as Sampled True-Time Delay Lines," Opt. Lett. **40**(4), 621–624 (2015).
5. X. S. Yao and L. Maleki, "Optoelectronic microwave oscillator," J. Opt. Soc. Am. B **13**(8), 1725–1735 (1996).
6. X. S. Yao and L. Maleki, "Multiloop optoelectronic oscillator," IEEE J. Quantum Electron. **36**(1), 79–84 (2000).
7. T. Bánky, B. Horváth, and T. Berceli, "Optimum configuration of multiloop optoelectronic oscillators," J. Opt. Soc. Am. B **23**(7), 1371–1380 (2006).
8. S. García and I. Gasulla, "Multi-cavity optoelectronic oscillators using multicore fibers," Opt. Express **23**(3), 2403–2415 (2015).
9. Z. Tang, S. Pan, D. Zhu, R. Guo, Y. Zhao, M. Pan, D. Ben, and J. Yao, "Tunable Optoelectronic Oscillator Based on a Polarization Modulator and a Chirped FBG," IEEE Photonics Technol. Lett. **24**(17), 1487–1489 (2012).
10. W. Li and J. Yao, "An optically tunable optoelectronic oscillator," J. Lightwave Technol. **28**(18), 2640–2645 (2010).
11. O. Lelièvre, V. Crozatier, G. Baili, P. Berger, G. Pillet, D. Dolfi, L. Morvan, F. Goldfarb, F. Bretenaker, and O. Llopis, "Ultra-low phase noise 10 GHz dual loop optoelectronic oscillator," in *Proceedings of IEEE 2016 Int. Topical Meeting on Microwave Photonics* (IEEE, 2016), pp. 106–109.
12. T. Mizuno, K. Shibahara, H. Ono, Y. Abe, Y. Miyamoto, F. Ye, T. Marioka, Y. Sasaki, Y. Amma, K. Takenaga, S. Matsuo, K. Aikawa, K. Saitoh, Y. Jung, D. J. Richardson, K. Pulverer, M. Bohn, and M. Yamada, "32-core dense SDM unidirectional transmission of PDM-16QAM signals over 1600 km using crosstalk-managed single-mode heterogeneous multicore transmission line," in *Optical Fiber Communication Conference*, (Optical Society of America, 2016), paper Th5C.3.
13. D. Eliyahu and L. Maleki, "Low phase noise and spurious level in multi-loop opto-electronic oscillators," in *Proceedings of IEEE International Frequency Control Symposium and PDA Exhibition Jointly with the 17th European Frequency and Time Forum* (IEEE, 2003), pp. 405–410.
14. K. Mikitchuk, A. Chizh, and S. Malyshev, "Modeling and design of delay-line optoelectronic oscillators," IEEE J. Quantum Electron. **52**(10), 1–8 (2016).
15. S. Pan, P. Zhou, Z. Tang, Y. Zhang, F. Zhang, and D. Zhu, "Optoelectronic Oscillator Based on Polarization Modulation," Fiber Integr. Opt. **34**(4), 185–203 (2015).

#302993 https://doi.org/10.1364/OE.25.023663
Journal © 2017 Received 21 Jul 2017; revised 13 Sep 2017; accepted 13 Sep 2017; published 18 Sep 2017

Optics EXPRESS

1. Introduction

Space division multiplexing technologies emerged as a solution to the problem of the capacity saturation of conventional singlemode fibers [1]. In particular, multicore fibers (MCFs) offer a compact medium to transmit several data signals simultaneously by providing multiple spatial paths. Despite MCFs were initially envisioned in the context of core and metro optical networks, they can also be applied to a wider range of application fields including radio access networks and multiple antenna connectivity, multi-parameter fiber sensing and Microwave Photonics signal processing [2–4]. Radiofrequency (RF) signal processing applications, such as microwave signal filtering, beamsteering in phased array antennas and arbitrary waveform generation, can benefit as well from the performance stability resulting from hosting all the signal samples under the same cladding, providing the same environmental and mechanical conditions for all the light paths. This advantage is particularly interesting in the case of multi-cavity optoelectronic oscillators (OEOs) [5–10,13–15], where the multiple cavities can be brought together by exploiting the spatial diversity of MCFs.

Introduced by Yao and Maleki in a single-cavity configuration [5], OEOs can generate RF signals with a low linewidth in a feedback-loop structure. A high spectral purity in single-cavity OEOs requires a long fiber loop, what translates into a large number of oscillation modes that are separated by a small frequency period. The selection of one oscillating frequency will thus require very selective RF filters. Dual-cavity OEOs were conceived to alleviate this narrowband RF filter requirement [6]. Particularly in [6], a short loop provides the required spectral separation between oscillating modes while a long loop is mainly responsible for the spectral purity. In general, the oscillation modes of a multi-cavity OEO are those where the oscillation frequencies of all the cavities in isolation overlap. On the other hand, the overall quality factor (and thus the spectral purity) is proportional to the sum of the cavity lengths weighted by the relative optical powers carried over them [7]. The number of loops can actually be generalized to an arbitrary number [7,8,13,14]. The work reported in [7] demonstrated 3-cavity OEOs by using 3 different fiber links whose lengths were multiple of a given reference value. In [8], we proposed and evaluated theoretically the implementation of multi-cavity OEOs where the cavities were provided by the different cores of the MCF.

We report here, for the first time to our knowledge, the experimental demonstration of multi-cavity OEOs implemented over a commercial homogeneous 7-core fiber. Two different architectures are demonstrated: unbalanced dual-cavity operation, where the cavity lengths are a multiple of a given reference value; and multi-cavity Vernier operation, where the cavity lengths are slightly different by exploiting the Vernier effect [9].

2. Experimental setup

We use a 20-m-long homogeneous 7-core fiber as the hosting medium for the multiple cavities that compose the OEO. This MCF, which is provided by Fibercore, is characterized by a cladding diameter of 125 μm, a core separation of 35 μm and a core mode field diameter of 6.4 μm. The fan-in/fan-out devices are provided by Optoscribe and have a maximum level of insertion loss of 2.5 dB in each way, including additional 1-dB losses due to the MCF splices. The measured intercore crosstalk, considering both the fan-in/fan-out devices and the MCF, is lower than −50 dB, low enough to assure independent cavity transmission.

2.1 Dual-cavity unbalanced OEO

As theoretically presented in [8], dual-cavity unbalanced OEO operation can be implemented in an N-core MCF if k_1 cores ($k_1 < N/2$) are linked to form the short cavity while the remaining N-k_1 cores comprise the long cavity. Figure 1 shows the experimental setup for dual-cavity unbalanced operation, where 3 different configurations were implemented: 1- and 6-core cavities ($k_1 = 1$) corresponding to 20- and 120-m cavities; 2- and 5-core cavities ($k_1 = 2$) corresponding to 40- and 100-m cavities; and 3- and 4-core cavities ($k_1 = 3$) corresponding

Optics EXPRESS

to 60- and 80-m cavities. To compensate for the optical losses, mainly due to the fan-in/fan-out devices, optical amplification stages of 20 and 40 dB were included, respectively, in the short and long loops. A 1-nm-bandwidth optical filter is placed at each loop before photodetection to suppress the residual phase noise of the Erbium Doped Fiber Amplifiers (EDFAs). After detection and RF amplification, a tunable RF filter centered at 4.5 GHz with a bandwidth of 5 MHz allows for single-mode oscillation. A power splitter is set at the output of the RF filter to allow the continuous monitoring of the RF spectrum. The cavity gain control is carried out by placing variable optical attenuators (VOAs) before photodetection.

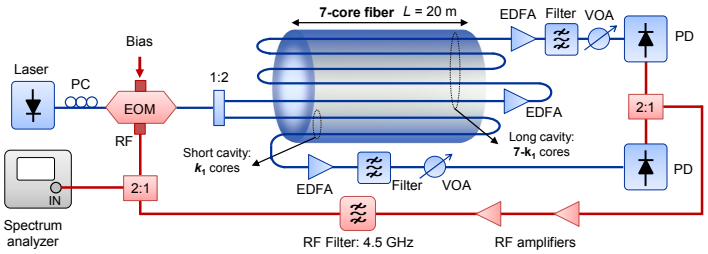

Fig. 1. Experimental setup for the dual-cavity unbalanced OEO over a 20-meter 7-core fiber. We demonstrated three different configurations: 1- and 6-core cavities (k_1 = 1), 2- and 5-core cavities (k_1 = 2), 3- and 4-core cavities (k_1 = 3). PC: polarization controller, RF: radiofrequency, EOM: electro-optic modulator, EDFA: Erbium-doped fiber amplifier, VOA: variable optical attenuator, PD: photodetector. Blue: optical path. Red: electrical path.

2.2 Multi-cavity Vernier OEO

A multi-cavity Vernier OEO can be implemented by using the N cores of the MCF as the corresponding N cavities that compose the oscillator. Figure 2 shows the experimental setup used to build a 3-cavity Vernier OEO with the 7-core fiber. Since we use a homogeneous MCF, the slightly different delays of the cavities can be obtained by adding an incremental length ΔL to each cavity, which can be done compactly by properly designing the physical length of each fan-in/fan-out arm [8]. For simplicity, we have used a 3-m standard singlemode fiber to produce the required incremental delay between cavities, and variable delay lines (VDLs) to finely adjust the length difference between cavities. Again, 20-dB optical amplification is included in each loop to compensate the insertion losses of the fan-in/fan-out devices. Once the signals have been photodetected, coupled together and amplified, a 4.4 to 5.0 GHz tunable RF filter with a 30-MHz bandwidth selects the desired oscillation frequency.

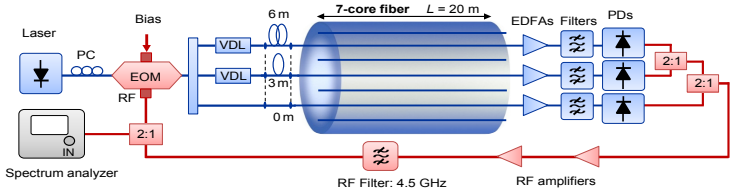

Fig. 2. Experimental setup for the multi-cavity Vernier OEO over a 7-core fiber. We compared both 2- and 3-cavity OEOs. PC: polarization controller, RF: radiofrequency, EOM: electro-optic modulator, VDL: variable delay line, EDFA: Erbium-doped fiber amplifier, VOA: variable optical attenuator, PD: photodetector. Blue: optical path. Red: electrical path.

3. Results and discussion

3.1 Oscillation frequencies

The oscillation frequencies of a multi-loop OEO verify $f_o = n_i/\tau_i$, for n_i = 1, 2,…, where i = 1, 2, …, N, being N the number of cavities, and τ_i is the time delay experienced in each cavity i including both the optical and the RF delays. In general, the resulting OEO oscillating modes

Optics EXPRESS

are those where the oscillation frequencies of all the cavities in isolation overlap. If the positive integers n_i are multiple of n_1 (where n_1 corresponds to the shortest cavity), the OEO oscillating frequencies coincide with the ones of the shortest cavity. For dual-loop unbalanced operation, the oscillation frequencies must verify for both the short and the long loops

$$f_o = \frac{m}{k_1\tau_g L + \tau_S}, \qquad f_o = \frac{n}{(N-k_1)\tau_g L + \tau_L}, \qquad m, n = 1, 2, \ldots, \tag{1}$$

where τ_g is the group delay per unit length of a single core of the MCF, L its length (L = 20 m), N the total number of cores (N = 7), while τ_S and τ_L are the residual time delays external to the MCF in the short and long cavities, respectively. In a similar way, the oscillation frequencies for the Vernier configuration verify [8],

$$f_o = \frac{n}{\Delta\tau}, \qquad n = 1, 2, \ldots, \tag{2}$$

being $\Delta\tau$ the incremental delay between cavities that produces the Vernier effect.

Figure 3 illustrates the measured RF oscillation spectra for the 3 dual-cavity unbalanced configurations around a central frequency of 4.5 GHz: (a, d) 1- and 6-core cavities (k_1 = 1); (b, e) 2- and 5-core cavities (k_1 = 2) and (c, f) 3- and 4-core cavities (k_1 = 3). The upper figures (a-c) show the spectrum of each individual cavity in isolation and the lower figures (d-f) the spectra for the dual-loop OEOs, each one for 3 consecutive oscillating frequencies given by 3 different frequency tuning positions of the RF filter (blue, yellow and orange curves). We see how the oscillating frequencies correspond to those modes that are, at the same time, fulfilling the oscillation conditions in the short and long loops, leading to a dual-loop spectrum periodicity of 6.7, 11.4, and 11.3 MHz, respectively for k_1 = 1, 2 and 3.

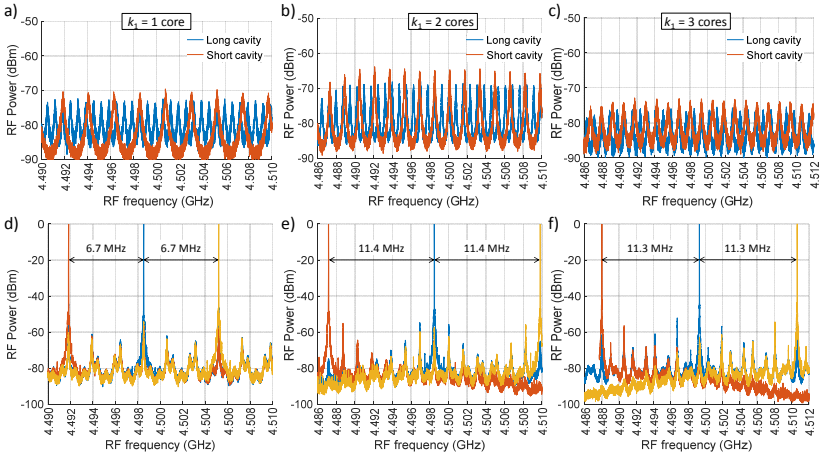

Fig. 3. Experimental oscillation spectra of a dual-cavity unbalanced OEO using a 20-meter 7-core fiber for three different configurations: (a, d) 1- and 6-core cavities (k_1 = 1); (b, e) 2- and 5-core cavities (k_1 = 2); (c, f) 3- and 4-core cavities (k_1 = 3). Upper figures correspond to the cavities in isolation and lower figures to the resulting dual-loop OEO.

We have also measured the oscillation frequencies of the 2- and 3-cavity Vernier OEOs. Figure 4(a) illustrates the measured spectrum for each isolated cavity, where we see, as expected, that the oscillation condition is not fulfilled as the open loop gain of each cavity is less than unity. With the help of the VDL placed at the first and second cavities, we matched the oscillating modes of all cavities at the frequency located near 4.494 GHz. The resulting spectrum of the oscillating mode at 4.494 GHz for both the 2- and 3-loop OEOs are compared in Fig. 4(b). An important reduction of 10 dB is observed at the spurious peaks corresponding

Optics EXPRESS

to the minor oscillating modes of the single cavities when increasing the number of cavities to 3. After finely adjusting the delay of each cavity, the single-loop delays are 499.2, 482.9, and 466.6 ns, respectively, for isolated cavities 1, 2 and 3. Figures 4(c) and 4(d) show 3 consecutive oscillating modes for the 2- and 3-loop Vernier configuration, respectively. As expected from Eq. (2), both the 2- and 3-cavity FSRs are identical with a value of 61 MHz. The 30-MHz RF filter bandwidth is then, by far, sufficiently narrow to allow single-mode oscillation for the Vernier OEO. We observe that increasing the number of cavities reduces the level of the minor oscillating modes of the single cavities.

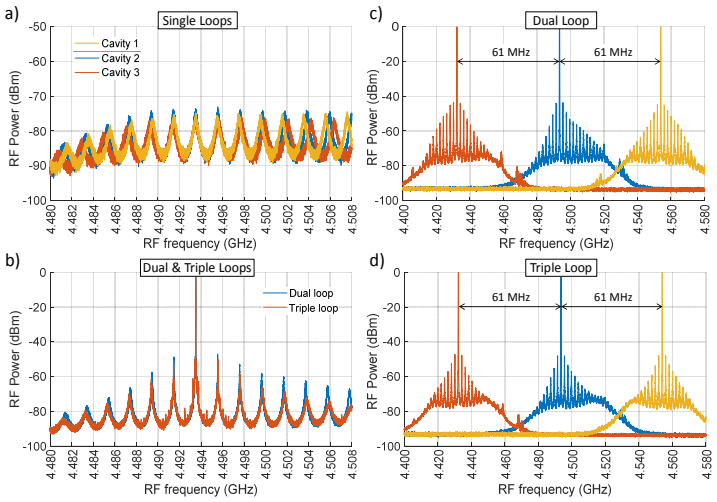

Fig. 4. Experimental oscillation spectra of a multi-cavity Vernier OEO using a 20-meter 7-core fiber for (a) each of the 3 cavities in isolation, (b) dual- versus triple-loop configurations, and 3 consecutive oscillation frequencies for (c) dual- and (d) triple-loop OEOs.

3.2 Phase noise

The measured phase noise spectrum for a representative case ($k_1 = 2$) of the unbalanced OEO is shown in the left part Fig. 5. As expected from [8], the measured phase noise of all 3 unbalanced configurations behave similarly. A phase noise around –90 dBc/Hz is achieved at a 10-kHz offset from the carrier, while it is downshifted below –125 dBc/Hz above 1 MHz. The high level of phase noise for frequency offsets below 10 kHz can be explained by different causes. First, possible fluctuations of the pump current applied to the EDFAs may contribute to the phase noise in the low-frequency region [10]. This is particularly important in the long cavity since it requires a double-stage EDFA. Moreover, the phase noise performance is degraded by fluctuations that may occur in both fiber loops and the RF delay, as well as by the lack of proper temperature stabilization. The spurs observed for frequency offsets above 1 MHz, corresponding to the minor oscillation modes, are below –95 dBc/Hz.

The right part of Fig. 5 shows the measured phase noise spectrum of both 2- and 3-cavity Vernier OEO configurations, which exhibit very similar responses. In both cases, a –85 dBc/Hz phase noise level is observed at a 10-kHz offset from the carrier, while it decreases down to –130 dBc/Hz for a 1-MHz offset. The main difference is the 10-dB reduction in the spurious peak level above 1 MHz (i.e., the minor oscillating modes of the single cavities) when the number of cavities increases from 2 to 3, as reported in [13,14]. This fact is related to the spectral purity of the oscillating mode, as we theoretically evaluated in [8].

Although the phase noise values of both unbalanced and Vernier schemes are, in principle, not comparable to those reported for ultra-low phase noise OEOs [11], they can be reduced by using low-residual phase noise components (RF amplifiers and photodetectors) and by reducing the optical losses and thus suppressing the need for optical amplifiers. In

Optics EXPRESS

addition, the phase noise performance can be improved if we use a laser with lower RIN and higher optical power, a Mach-Zehnder modulator with a lower V_π value or a photodiode with better responsivity [11]. Although the use of 1-nm-bandwidth optical filtering reduces the ASE noise induced by the EDFAs, we still observe a considerable noise level. This is observed more clearly in the unbalanced configuration since a double-stage EDFA amplification is placed in the long loop. In the multi-cavity Vernier OEO, the spectral purity of the oscillation can be improved by increasing the number of cavities, while the phase noise level can be further diminished increasing the MCF length. As opposed to single-cavity OEOs, this will not alter the FSR of the OEO that will actually be preserved by the Vernier effect, as Eq. (2) shows. In contrast, the unbalanced OEO could not benefit from a fiber length increase since it is configured using a relatively small number of cores and, therefore, it is inherently linked to shorter cavity lengths to avoid the use of RF filters with extremely high selectivity. In that case, by increasing the number of cores up to 32, such as the latest reported dense-core MCFs [12], the length of the long cavity could be considerably increased as compared to the short one, improving as a consequence the phase noise performance.

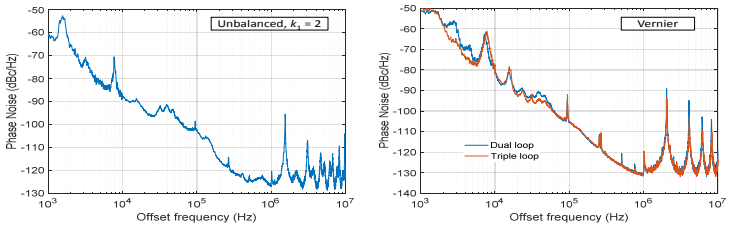

Fig. 5. Experimental phase noise of the multi-cavity OEO for (Left) dual-cavity unbalanced OEO with 2- and 5-core cavities ($k_1 = 2$), and (Right) 2- and 3-cavity Vernier configurations.

4. Conclusions

By exploiting the spatial diversity inherent to MCFs, we have demonstrated, for the first time to our knowledge, the implementation of multi-cavity OEOs where the different optical loops are provided by the different cores of the MCF. A set of OEOs has been experimentally proved over a commercial 7-core fiber using both unbalanced 2-cavity and multi-cavity Vernier OEO operation. Since all the cavities are hosted within the same cladding, this approach provides a fiber integrated medium for enhancing the OEO relative stability against environmental and mechanical fluctuations. Microwave Photonics will benefit from the compactness and spatial parallelism of the reported OEOs that allow high-spectral purity oscillation using moderate cavity lengths around 20 m without the need of selective RF filters. We must take into account that the requirement for loss compensation by means of EDFA amplification might compromise the potential feature of reduced footprint. This can be circumvent by replacing the EDFAs by compact reflective semiconductor optical amplifiers, by reducing the optical losses or by introducing an optical source emitting higher optical power. In addition, in the particular case of the dual-loop OEOs, polarization modulation and multiplexing could be used to improve the length and polarization stabilities, as well as to reduce the cost and the residual phase noise since a single photodetector is used for both cavities [15].

Funding

H2020 European Research Council (ERC) (724663); Ministerio de Economía y Competitividad (TEC2014-60378-C2-1-R, TEC2016-80150-R, BES-2015-073359, RYC-2014-16247).

Acknowledgments

We thank Javier Hervas, Javier Madrigal and Prof. Salvador Sales for their collaboration.